DEVELOPMENT AND IMPLEMENTATION OF ? T PROCEDURE FOR THE SNS LINAC

S.Bragin, A.Feschenko, Yu.Kisselev, L.Kravchuk, O.Volodkevich (INR, Moscow)
A.Aleksandrov, J.Galambos, S.Henderson, A.Shishlo (ORNL/SNS)

The ? t procedure was proposed and developed by K.R. Crandall [1] for adjusting the rf phases and amplitudes throughout the 805-MHz LAMPF Linac. The present report is devoted to development and implementation of the procedure at the SNS CCL Linac as well as the first results of its experimental use. The work is based on fundamental ideas of K.R.Crandall as well on experience obtained during commissioning and initial operation of the INR Linac [2].

The SNS CCL accelerator operates at 805MHz. It includes four CCL Modules (Side Coupled Structure) and provides acceleration of H-minus beam from 86.8 MeV up to 185.6 MeV. Each Module consists of twelve segments. Phase velocity of accelerating field is constant within the segment and changes stepwise from segment to segment. Strip line beam position monitors (BPM), operating at a frequency of the upstream DTL Linac 402.5 MHz are installed in inter segment sections and are used as beam phase probes.

Theoretical considerations.

In ? t procedure the bunch of the accelerating beam is treated as a single particle executing a linear motion in *(?f , ?W)* phase plane. Normally the motion is linear in the vicinity of a synchronous particle. Though there is no synchronous particle in CCL module, nevertheless the motion can be considered to be linear with respect to a design particle. In this case all the formal considerations on linear motion are applicable. One should note, that linear motion requirements imply limitation on deviations from nominal values of rf phase and amplitude as well as of beam energy.

The ? t procedure can be explained referring to fig. 1. The information about the phase and amplitude of accelerating field in cavity N (in case of SNS CCL Linac N=1,2,3,4) can be derived by

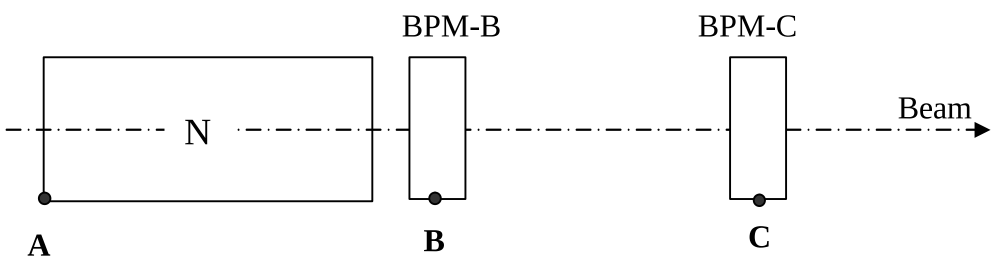

Fig. 1 Explanation of ? t procedure.

processing phases of signals induced by the beam in BPM-B and BPM-C with respect to accelerator reference line and comparing the results with the results of beam dynamics simulations. The point A in fig. 1 corresponds to physical entrance of the cavity. Points B and C correspond to longitudinal coordinates of beam phase probes. In case of SNS BPMs, representing shortened strip lines, the longitudinal positions of signal connectors must be assigned to the above coordinated. Longitudinal positions of points B and C essentially influence an accuracy of ? t procedure. Normally phase probes located at the exit the module and at the exit of the next module are used. However, another probe positions are possible that is why ? t procedure parameters have been calculated for different BPMs combinations.

Let t_{AB} and t_{AC} be the times of flight from point A to points B and C correspondingly. The values of interest are the differences of times of flight for the rf field off and on:

$$t_B = t_{ABoff} - t_{ABon}$$

$$t_C = t_{ACoff} - t_{ACon}$$

Typical values of t_B and t_C are hundreds and even thousands of degrees that is why the use of deviations with respect to design values is reasonable:

$$\Delta t_B = (t_{ABoff} - t_{ABon}) - (t_{ABoff,des} - t_{ABon,des})$$

$$\Delta t_C = (t_{ACoff} - t_{ACon}) - (t_{ACoff,des} - t_{ACon,des})$$

Here $t_{ABoff,des}$, $t_{ABon,des}$, $t_{ACoff,des}$ and $t_{ACon,des}$ are the values of t_{ABoff}, t_{ABon} , t_{ACoff} and t_{ACon} for nominal amplitude and phase as well as the nominal energy at the entrance of the cavity.

It can be shown [1] that in the vicinity of the design particle the parameters ?t_B and ?t_C linearly depend on deviation of energy ?W_A and phase ?f_A with respect to nominal values at the entrance of the cavity:

$$\begin{pmatrix} \Delta t_B \\ \Delta t_C \end{pmatrix} = T \begin{pmatrix} \Delta j_A \\ \Delta W_A \end{pmatrix}$$

If the values of ?t_B and ?t_C are known, then the deviations ?W_A and ?f_A can be found:

$$\begin{pmatrix} \Delta j_A \\ \Delta W_A \end{pmatrix} = A_t \begin{pmatrix} \Delta t_B \\ \Delta t_C \end{pmatrix},$$

where $A_t = T^{-1}$. In practice the changes of phase of the induced in BPMs signals rather than the changes of time of flight are measured. If $\Delta j_1 = w \cdot \Delta t_B$ and $\Delta j_2 = w \cdot \Delta t_C$, where ? is an operating frequency of BPMs, then

$$\begin{pmatrix} \Delta j_A \\ \Delta W_A \end{pmatrix} = A \begin{pmatrix} \Delta j_1 \\ \Delta j_2 \end{pmatrix}$$

or

$$\begin{cases} \Delta j_A = a_{11} \cdot \Delta j_1 + a_{12} \cdot \Delta j_2 \\ \Delta W_A = a_{21} \cdot \Delta j_1 + a_{22} \cdot \Delta j_2 \end{cases},$$

where $A = \frac{1}{w} \cdot A_t$.

The elements of the transformation matrixes depend on the amplitude of accelerating field and this feature can be used to find the amplitude. In practice a more convenient way to find the amplitude is by comparing the slope of theoretical and experimental lines, generated in *(?f_1,?f_2)* plane, when the entrance phase ?f_A is varied.

If the phase of rf field is varied than the experimental points in *(?f_1,?f_2)* plane will be located on a so called phase variable line, defined by the equation

$$a_{21} \cdot \Delta j_1 + a_{22} \cdot \Delta j_2 = \Delta W_A = const, \qquad (1)$$

each point of the line univocally corresponding to phase deviation ?f_A at the entrance of the cavity.

If the phase is nominal, then

$$a_{11} \cdot \Delta j_1 + a_{12} \cdot \Delta j_2 = \Delta j_A = 0 \text{ or } \Delta j_2 = -\frac{a_{11}}{a_{12}} \cdot \Delta j_1. \qquad (2)$$

One should note that the line (1) can be found experimentally by measuring ?f_1 and ?f_2 versus cavity phase while the line (2) is a theoretical one. Each point of line (2) corresponds to a certain value of ?W_A.

The point of intersection of experimental line (1) and theoretical one (2) defines deviation of phase $?f_A$ and energy $?W_A$ at the entrance of the cavity with respect to nominal values.

Design parameters

To implement a ? t procedure the following design parameters are required:

- ($f_{ABoff,des}$- $f_{ABon,des}$) and ($f_{ACoff,des}$ - $f_{ACon,des}$);
- $arctg\left(\frac{d(\Delta j_2)}{d(\Delta j_1)}\right)$ for different amplitudes of accelerating field;
- matrix *A* elements for different amplitudes.

To above parameters have been derived by simulating single particle beam dynamics in CCL modules. Figures 2÷4 show the lines in *($?f_1$,$?f_2$)* plane for particular BPM combination. The values of $?f_1$ and $?f_2$ correspond to operating frequency of BPMs 402.5 MHz. Three sets of lines are displayed in each figure: for the nominal input energy and for the energies differing by ±50 keV. The amplitude is varied from -5% to +5% with respect to nominal value with a step of 1%. Points on the lines correspond to different input phases with a step of 2.5° (*f*=805 MHz). Nominal input phase for CCL Module #1 has been selected to provide intersection of the lines corresponding to nominal energy of 86.8277 MeV at the center of coordinates to be equal to -30.70°. For the subsequent modules the nominal phase has been selected similarly for input energies calculated for selected nominal parameters in previous modules. The nominal phases for the second and the third modules have been thus selected -30.77° and -30.28°.

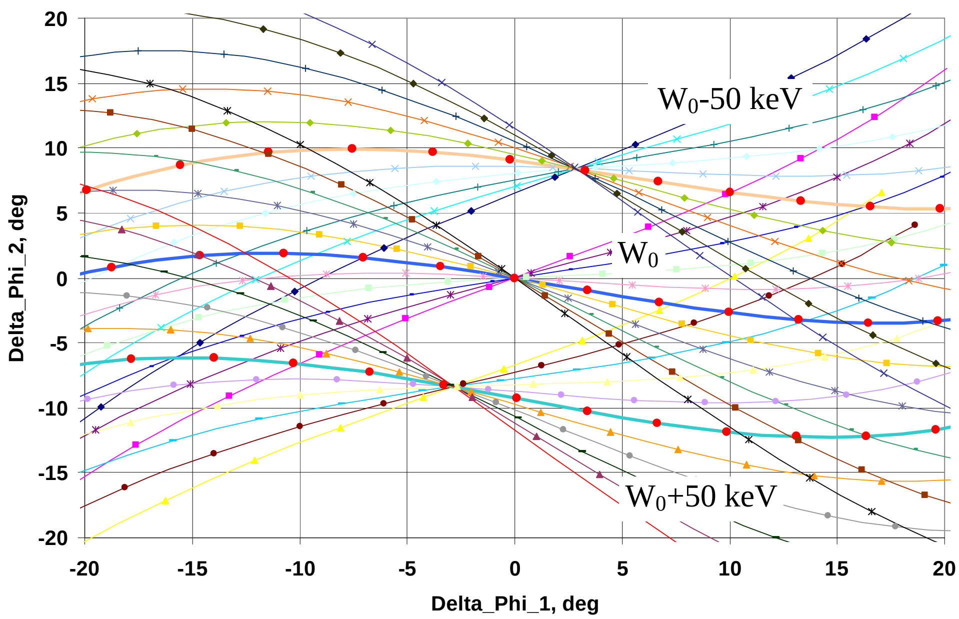

Fig. 2 Behavior of lines in *($?f_1$,$?f_2$)* plane for CCL Module #1 (BPM 112, BPM 212)

The ? t procedure parameters for CCL Modules 1÷3 for different BPM combinations are summarized in Tables 1÷3. The sensitivity of the slope of a line in *($?f_1$,$?f_2$)* plane to amplitude variation can be used to compare the accuracy of amplitude setting for different BPM combinations (Table 4). However these estimates are very relative as neither beam debunching nor real stability is taken into account.

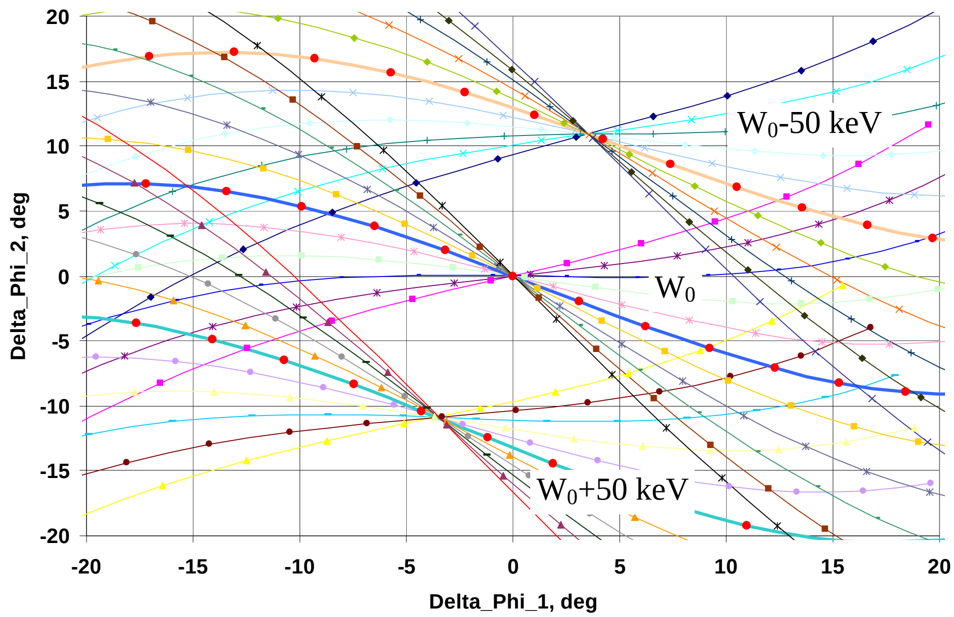

Fig. 3 Behavior of lines in *(?f 1,?f 2)* plane for CCL Module #2 (BPM 212, BPM 312)

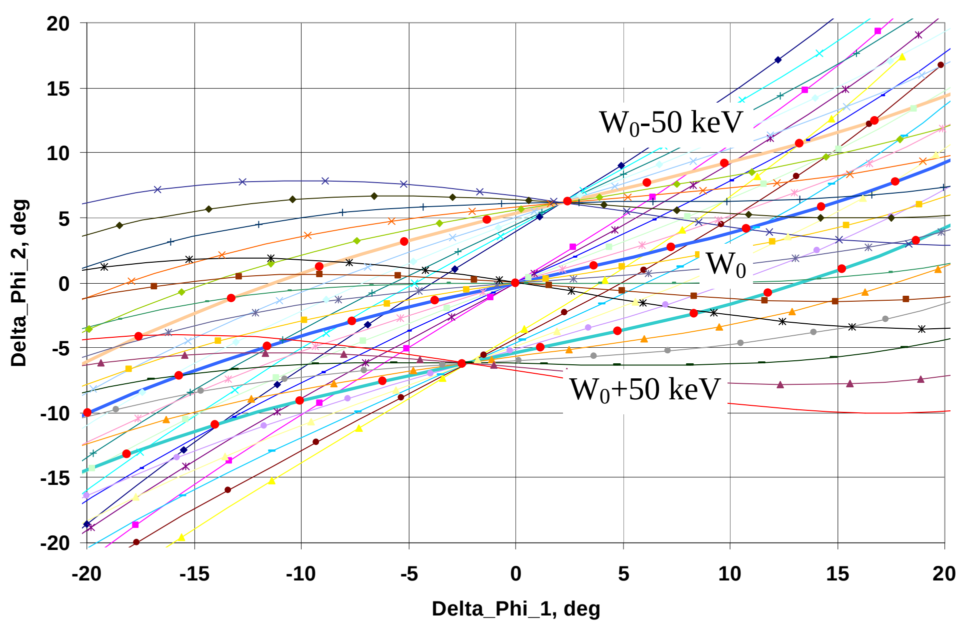

Fig. 4 Behavior of lines in *(?f 1,?f 2)* plane for CCL Module #3 (BPM 312, BPM 411)

Table 1. Calculated parameters for CCL module #1.

BPM-A BPM-B	Parameter	Units	Amplitude E/E_0										
			0.95	**0.96**	**0.97**	**0.98**	**0.99**	**1.00**	**1.01**	**1.02**	**1.03**	**1.04**	**1.05**
112 212	$arctg\left(\frac{d(\Delta j_2)}{d(\Delta j_1)}\right)$	deg	25.92	14.14	1.51	-11.15	-22.43	-31.87	-39.63	-45.84	-50.89	-54.89	-58.19
	a_{11}		7.90430E-01	7.45012E-01	7.08563E-01	6.78538E-01	6.53559E-01	6.30970E-01	6.11873E-01	5.94844E-01	5.79888E-01	5.67477E-01	5.54894E-01
	a_{12}		-2.94337E-01	-2.82019E-01	-2.72893E-01	-2.66618E-01	-2.62051E-01	-2.58164E-01	-2.55593E-01	-2.53840E-01	-2.53464E-01	-2.53240E-01	-2.53750E-01
	a_{21}	eV/rad	1.58843E+05	7.43172E+04	7.13255E+03	-4.91620E+04	-9.59965E+04	-1.35893E+05	-1.71110E+05	-2.02217E+05	-2.30056E+05	-2.55021E+05	-2.77339E+05
	a_{22}	eV/rad	-3.26885E+05	-2.94964E+05	-2.69940E+05	-2.49510E+05	-2.32548E+05	-2.18633E+05	-2.06614E+05	-1.96370E+05	-1.87041E+05	-1.79335E+05	-1.72075E+05
	$(f_{ABoff,des} - f_{ABon,des})$	deg						652.22					
	$(f_{ACoff,des} - f_{ACon,des})$	deg						2041.66					
112 302	$arctg\left(\frac{d(\Delta j_2)}{d(\Delta j_1)}\right)$	deg	21.60	7.02	-8.10	-22.03	-33.43	-42.18	-49.00	-54.17	-58.32	-61.57	-64.22
	a_{11}		7.46581E-01	7.03514E-01	6.68305E-01	6.39233E-01	6.14534E-01	5.92407E-01	5.73474E-01	5.57046E-01	5.42083E-01	5.29695E-01	5.17038E-01
	a_{12}		-2.50530E-01	-2.40214E-01	-2.32277E-01	-2.26951E-01	-2.23016E-01	-2.19686E-01	-2.17386E-01	-2.16086E-01	-2.15756E-01	-2.15457E-01	-2.15879E-01
	a_{21}	eV/rad	1.10145E+05	3.09144E+04	-3.26899E+04	-8.59454E+04	-1.30628E+05	-1.68551E+05	-2.02151E+05	-2.31457E+05	-2.57953E+05	-2.81777E+05	-3.03010E+05
	a_{22}	eV/rad	-2.78234E+05	-2.51240E+05	-2.29763E+05	-2.12389E+05	-1.97908E+05	-1.86046E+05	-1.75729E+05	-1.67164E+05	-1.59215E+05	-1.52578E+05	-1.46393E+05
	$(f_{ABoff,des} - f_{ABon,des})$	deg						652.22					
	$(f_{ACoff,des} - f_{ACon,des})$	deg						2284.48					
202 212	$arctg\left(\frac{d(\Delta j_2)}{d(\Delta j_1)}\right)$	deg	27.91	15.96	1.79	-13.72	-28.05	-40.09	-49.54	-56.76	-62.48	-66.78	-70.27
	a_{11}		9.42155E-01	8.86408E-01	8.44296E-01	8.08786E-01	7.77085E-01	7.52387E-01	7.28527E-01	7.08029E-01	6.91539E-01	6.75911E-01	6.62297E-01
	a_{12}		-4.46519E-01	-4.24064E-01	-4.09027E-01	-3.96970E-01	-3.86678E-01	-3.79324E-01	-3.72973E-01	-3.67426E-01	-3.64630E-01	-3.62256E-01	-3.60434E-01
	a_{21}	eV/rad	1.89333E+05	8.84219E+04	8.49887E+03	-5.85987E+04	-1.14140E+05	-1.62043E+05	-2.03732E+05	-2.40694E+05	-2.74351E+05	-3.03751E+05	-3.31019E+05
	a_{22}	eV/rad	-3.57467E+05	-3.09134E+05	-2.71310E+05	-2.40066E+05	-2.14242E+05	-1.92538E+05	-1.73789E+05	-1.57756E+05	-1.42939E+05	-1.30343E+05	-1.18754E+05
	$(f_{ABoff,des} - f_{ABon,des})$	deg						875.59					
	$(f_{ACoff,des} - f_{ACon,des})$	deg						2041.66					
202 302	$arctg\left(\frac{d(\Delta j_2)}{d(\Delta j_1)}\right)$	deg	23.34	7.95	-9.57	-26.63	-40.43	-50.82	-58.45	-64.02	-68.42	-71.72	-74.40
	a_{11}		8.65077E-01	8.14192E-01	7.74378E-01	7.40951E-01	7.10507E-01	6.86707E-01	6.63679E-01	6.44708E-01	6.28485E-01	6.13331E-01	5.99907E-01
	a_{12}		-3.69466E-01	-3.51346E-01	-3.38554E-01	-3.28604E-01	-3.19992E-01	-3.13787E-01	-3.08333E-01	-3.04131E-01	-3.01756E-01	-2.99621E-01	-2.98090E-01
	a_{21}	eV/rad	1.27627E+05	3.57778E+04	-3.78784E+04	-9.96215E+04	-1.51028E+05	-1.95381E+05	-2.33949E+05	-2.67882E+05	-2.99068E+05	-3.26268E+05	-3.51575E+05
	a_{22}	eV/rad	-2.95780E+05	-2.56124E+05	-2.24565E+05	-1.98721E+05	-1.77294E+05	-1.59273E+05	-1.43670E+05	-1.30580E+05	-1.18292E+05	-1.07806E+05	-9.82133E+04
	$(f_{ABoff,des} - f_{ABon,des})$	deg						875.59					
	$(f_{ACoff,des} - f_{ACon,des})$	deg						2284.48					

Table 2. Calculated parameters for CCL module #2.

BPM-A BPM-B	Parameter	Units	Amplitude E/E_0										
			0.95	**0.96**	**0.97**	**0.98**	**0.99**	**1.00**	**1.01**	**1.02**	**1.03**	**1.04**	**1.05**
212 312	$arctg\left(\frac{d(\Delta j_2)}{d(\Delta j_1)}\right)$	deg	35.88	27.28	17.42	6.53	-4.43	-14.92	-24.31	-32.32	-39.22	-44.65	-49.28
	a_{11}		8.34817E-01	7.84033E-01	7.44656E-01	7.11904E-01	6.83529E-01	6.59556E-01	6.39697E-01	6.20802E-01	6.06274E-01	5.91138E-01	5.78301E-01
	a_{12}		-3.08263E-01	-2.92642E-01	-2.82568E-01	-2.73619E-01	-2.66743E-01	-2.62665E-01	-2.59046E-01	-2.55527E-01	-2.54350E-01	-2.53577E-01	-2.52301E-01
	a_{21}	eV/rad	3.44818E+05	2.20698E+05	1.22547E+05	4.11468E+04	-2.59289E+04	-8.35414E+04	-1.33525E+05	-1.77225E+05	-2.17358E+05	-2.51480E+05	-2.83588E+05
	a_{22}	eV/rad	-4.76660E+05	-4.28045E+05	-3.90667E+05	-3.59680E+05	-3.34346E+05	-3.13612E+05	-2.95571E+05	-2.80129E+05	-2.66357E+05	-2.54585E+05	-2.44132E+05
	$(f_{ABoff,des} - f_{ABon,des})$	deg						629.20					
	$(f_{ACoff,des} - f_{ACon,des})$	deg						1911.17					
212 402	$arctg\left(\frac{d(\Delta j_2)}{d(\Delta j_1)}\right)$	deg	33.97	23.33	10.98	-2.15	-14.75	-25.93	-35.23	-42.50	-48.49	-53.20	-56.97
	a_{11}		7.88658E-01	7.40701E-01	7.02649E-01	6.71867E-01	6.44330E-01	6.20690E-01	6.00882E-01	5.82832E-01	5.68687E-01	5.53080E-01	5.40811E-01
	a_{12}		-2.62467E-01	-2.49432E-01	-2.40467E-01	-2.33097E-01	-2.27470E-01	-2.23823E-01	-2.20693E-01	-2.17912E-01	-2.16999E-01	-2.15881E-01	-2.14950E-01
	a_{21}	eV/rad	2.73443E+05	1.57317E+05	6.44694E+04	-1.14829E+04	-7.50622E+04	-1.29946E+05	-1.77813E+05	-2.18850E+05	-2.56720E+05	-2.89690E+05	-3.19864E+05
	a_{22}	eV/rad	-4.05847E+05	-3.64842E+05	-3.32460E+05	-3.06413E+05	-2.85120E+05	-2.67236E+05	-2.51810E+05	-2.38893E+05	-2.27243E+05	-2.16739E+05	-2.07991E+05
	$(f_{ABoff,des} - f_{ABon,des})$	deg						629.20					
	$(f_{ACoff,des} - f_{ACon,des})$	deg						2133.86					
302 312	$arctg\left(\frac{d(\Delta j_2)}{d(\Delta j_1)}\right)$	deg	37.13	29.24	19.42	7.60	-5.36	-18.53	-30.55	-40.74	-48.98	-55.54	-60.81
	a_{11}		9.96800E-01	9.36717E-01	8.87344E-01	8.48019E-01	8.14597E-01	7.87017E-01	7.62958E-01	7.41291E-01	7.20379E-01	7.05333E-01	6.90061E-01
	a_{12}		-4.71103E-01	-4.45432E-01	-4.25523E-01	-4.10736E-01	-3.98784E-01	-3.90057E-01	-3.82491E-01	-3.75940E-01	-3.70611E-01	-3.67859E-01	-3.64609E-01
	a_{21}	eV/rad	4.11724E+05	2.63678E+05	1.46029E+05	4.90140E+04	-3.09008E+04	-9.96861E+04	-1.59254E+05	-2.11621E+05	-2.58266E+05	-3.00061E+05	-3.38393E+05
	a_{22}	eV/rad	-5.43920E+05	-4.71054E+05	-4.14193E+05	-3.67605E+05	-3.29337E+05	-2.97476E+05	-2.69804E+05	-2.45754E+05	-2.24676E+05	-2.05968E+05	-1.89059E+05
	$(f_{ABoff,des} - f_{ABon,des})$	deg						836.30					
	$(f_{ACoff,des} - f_{ACon,des})$	deg						1911.17					
302 402	$arctg\left(\frac{d(\Delta j_2)}{d(\Delta j_1)}\right)$	deg	35.19	25.09	12.30	-2.50	-17.67	-31.46	-42.70	-51.27	-57.86	-63.11	-67.13
	a_{11}		9.14961E-01	8.60127E-01	8.14054E-01	7.78390E-01	7.46685E-01	7.20061E-01	6.96524E-01	6.76455E-01	6.57096E-01	6.41314E-01	6.27226E-01
	a_{12}		-3.89733E-01	-3.69013E-01	-3.52075E-01	-3.40316E-01	-3.30683E-01	-3.23141E-01	-3.16704E-01	-3.11619E-01	-3.07473E-01	-3.04343E-01	-3.01919E-01
	a_{21}	eV/rad	3.17235E+05	1.82682E+05	7.46910E+04	-1.33035E+04	-8.69862E+04	-1.50750E+05	-2.06115E+05	-2.54005E+05	-2.96630E+05	-3.35905E+05	-3.70974E+05
	a_{22}	eV/rad	-4.49973E+05	-3.90240E+05	-3.42700E+05	-3.04580E+05	-2.73096E+05	-2.46443E+05	-2.23398E+05	-2.03707E+05	-1.86400E+05	-1.70405E+05	-1.56552E+05
	$(f_{ABoff,des} - f_{ABon,des})$	deg						836.30					
	$(f_{ACoff,des} - f_{ACon,des})$	deg						2133.86					

Table 3. Calculated parameters for CCL module #3.

BPM-A BPM-B	Parameter	Units	Amplitude E/E_0										
			0.95	**0.96**	**0.97**	**0.98**	**0.99**	**1.00**	**1.01**	**1.02**	**1.03**	**1.04**	**1.05**
312 411	$arctg\left(\frac{d(\Delta j_2)}{d(\Delta j_1)}\right)$	deg	46.23	42.10	37.51	32.33	26.61	20.26	13.61	6.65	-0.48	-7.46	-14.04
	a_{11}		9.94526E-01	9.35453E-01	8.90860E-01	8.53166E-01	8.18599E-01	7.87879E-01	7.63671E-01	7.40480E-01	7.20939E-01	7.02397E-01	6.84788E-01
	a_{12}		-3.72797E-01	-3.52184E-01	-3.37336E-01	-3.26997E-01	-3.17030E-01	-3.08616E-01	-3.03883E-01	-2.98760E-01	-2.94397E-01	-2.90958E-01	-2.87739E-01
	a_{21}	eV/rad	8.19997E+05	6.42963E+05	5.01486E+05	3.83824E+05	2.84146E+05	1.96601E+05	1.22140E+05	5.59187E+04	-3.83386E+03	-5.72950E+04	-1.05004E+05
	a_{22}	eV/rad	-7.85543E+05	-7.11715E+05	-6.53488E+05	-6.06396E+05	-5.67207E+05	-5.32592E+05	-5.04710E+05	-4.79723E+05	-4.57187E+05	-4.37696E+05	-4.20016E+05
	$(f_{ABoff,des} - f_{ABon,des})$	deg						533.41					
	$(f_{ACoff,des} - f_{ACon,des})$	deg						1535.06					
312 409	$arctg\left(\frac{d(\Delta j_2)}{d(\Delta j_1)}\right)$	deg	45.99	42.66	39.06	35.08	30.74	26.03	21.01	15.76	10.22	4.66	-0.88
	a_{11}		1.08018E+00	1.01618E+00	9.68668E-01	9.29132E-01	8.91669E-01	8.59512E-01	8.33769E-01	8.09309E-01	7.88664E-01	7.69686E-01	7.51283E-01
	a_{12}		-4.58706E-01	-4.32969E-01	-4.14960E-01	-4.02909E-01	-3.89960E-01	-3.80018E-01	-3.74058E-01	-3.67294E-01	-3.61942E-01	-3.58111E-01	-3.54360E-01
	a_{21}	eV/rad	1.00048E+06	8.06101E+05	6.52217E+05	5.24697E+05	4.14878E+05	3.20221E+05	2.38564E+05	1.66438E+05	1.01340E+05	4.39296E+04	-7.94044E+03
	a_{22}	eV/rad	-9.66568E+05	-8.74972E+05	-8.03861E+05	-7.47168E+05	-6.97688E+05	-6.55813E+05	-6.21261E+05	-5.89768E+05	-5.62082E+05	-5.38716E+05	-5.17263E+05
	$(f_{ABoff,des} - f_{ABon,des})$	deg						533.41					
	$(f_{ACoff,des} - f_{ACon,des})$	deg						1348.53					
402 409	$arctg\left(\frac{d(\Delta j_2)}{d(\Delta j_1)}\right)$	deg	45.74	43.17	40.21	36.93	33.16	28.84	23.92	18.52	12.37	5.80	-1.13
	a_{11}		1.37529E+00	1.30117E+00	1.23680E+00	1.18962E+00	1.14173E+00	1.10163E+00	1.06537E+00	1.03555E+00	1.00734E+00	9.80614E-01	9.60907E-01
	a_{12}		-7.55467E-01	-7.17043E-01	-6.84013E-01	-6.62809E-01	-6.37939E-01	-6.20292E-01	-6.05419E-01	-5.91165E-01	-5.79185E-01	-5.70632E-01	-5.63378E-01
	a_{21}	eV/rad	1.27382E+06	1.03217E+06	8.32754E+05	6.71798E+05	5.31228E+05	4.10424E+05	3.04832E+05	2.12965E+05	1.29438E+05	5.59682E+04	-1.01560E+04
	a_{22}	eV/rad	-1.24143E+06	-1.10032E+06	-9.85018E+05	-8.93939E+05	-8.13069E+05	-7.45330E+05	-6.87460E+05	-6.35809E+05	-5.89996E+05	-5.50845E+05	-5.15054E+05
	$(f_{ABoff,des} - f_{ABon,des})$	deg						711.07					
	$(f_{ACoff,des} - f_{ACon,des})$	deg						1348.53					
402 411	$arctg\left(\frac{d(\Delta j_2)}{d(\Delta j_1)}\right)$	deg	45.98	42.61	38.65	34.11	28.83	22.60	15.61	7.88	-0.58	-9.26	-17.80
	a_{11}		1.20445E+00	1.13846E+00	1.08115E+00	1.03763E+00	9.96254E-01	9.59268E-01	9.27567E-01	9.00786E-01	8.75698E-01	8.50747E-01	8.32401E-01
	a_{12}		-5.84018E-01	-5.54359E-01	-5.28532E-01	-5.10981E-01	-4.92944E-01	-4.78529E-01	-4.67528E-01	-4.57162E-01	-4.48008E-01	-4.40760E-01	-4.34764E-01
	a_{21}	eV/rad	9.93078E+05	7.82498E+05	6.08603E+05	4.66811E+05	3.45812E+05	2.39368E+05	1.48353E+05	6.80244E+04	-4.65684E+03	-6.93959E+04	-1.27639E+05
	a_{22}	eV/rad	-9.59697E+05	-8.50676E+05	-7.61117E+05	-6.89167E+05	-6.28269E+05	-5.74990E+05	-5.30883E+05	-4.91685E+05	-4.56371E+05	-4.25476E+05	-3.97472E+05
	$(f_{ABoff,des} - f_{ABon,des})$	deg						711.07					
	$(f_{ACoff,des} - f_{ACon,des})$	deg						1535.06					

Table 4. Amplitude sensitivity of the slope angle in the vicinity of nominal amplitude.

CCL Module #	Amplitude sensitivity, deg/% for different BPMs			
1	BPM 112 BPM 212	BPM 112 BPM 302	BPM 202 BPM 212	BPM 202 BPM 302
	8.6	7.985	10.745	9.01
2	BPM 212 BPM 312	BPM 212 BPM 402	BPM 302 BPM 312	BPM 302 BPM 402
	9.94	10.24	12.595	12.515
3	BPM 312 BPM 411	BPM 312 BPM 409	BPM 402 BPM 409	BPM 402 BPM 411
	6.5	4.73	4.63	6.61

Implementation of ? t procedure.

To carry out a ? t procedure phase signals from two BPMs are measured for several phases f_c of CCL Module with the field on, as well as these two signals with the field off. Then the values of $?f_1$ and $?f_2$ are calculated. The points in $(?f_1, ?f_2)$ plane are rms fitted by linear functions of f_c:

$$\begin{cases} \Delta j_1 = k_1 \cdot j_c + b_1 \\ \Delta j_2 = k_2 \cdot j_c + b_2 \end{cases}$$

The above functions can be treated as parametric equation of a line in $(?f_1, ?f_2)$ plane:

$$\Delta j_2 = k \cdot \Delta j_1 + b\,, \tag{3}$$

where $k = \frac{k_2}{k_1}$, $b = \frac{b_2 \cdot k_1 - b_1 \cdot k_2}{k_1}$. The slope of this line $arctg(k)$ is compared with the calculated values (Tables 1÷3) thus enabling to determine the amplitude of accelerating field. Each point of the line (3) corresponds to a definite phase of accelerating field f_c. Nominal phase can be found as a solution of system of two equations (2) and (3):

$$j_{cS} = -\frac{b_1 \cdot a_{11} + b_2 \cdot a_{12}}{k_1 \cdot a_{11} + k_2 \cdot a_{12}}$$

The corresponding values of $?f_1$ and $?f_2$ can be found as:

$$(\Delta j_1)_S = k_1 \cdot j_{cS} + b_1$$
$$(\Delta j_2)_S = k_2 \cdot j_{cS} + b_2$$

Deviation of energy at the entrance of the cavity can be found by substituting the determined values of $(?f_1)_S$ and $(?f_2)_S$ in (1):

$$\Delta W_A = \frac{b_2 \cdot k_1 - b_1 \cdot k_2}{k_1 \cdot a_{11} + k_2 \cdot a_{12}} \cdot (a_{11} \cdot a_{22} - a_{12} \cdot a_{21})$$

Data acquisition is done with the code DeltaT 1Dscan. During the measurements the cavity (cavities) located between BPM-B and BPM-C must be turned off. To collect the data two scans must be done. The first scan is done with the tuned cavity turned on and the second one - with turned off. The results are written in text file.

Data processing is done with the LabVIEW code dtProcedure6.vi (for LabVIEW 6.1) or dtProcedure7.vi (for LabVIEW 7.1). The display of dTProcedure Labview 6.1 window is shown in fig. 5. Depending on the position of the switch **Data File Loading – Current Data Processing** the user can either load a new data file or process already loaded data.

Two plots in the left part of the window represent the measured functions $?f_1$ (f_c) and $?f_2(f_c)$. The central plot represents a $(?f_1, ?f_2)$ plane. This plot shows experimental points and a

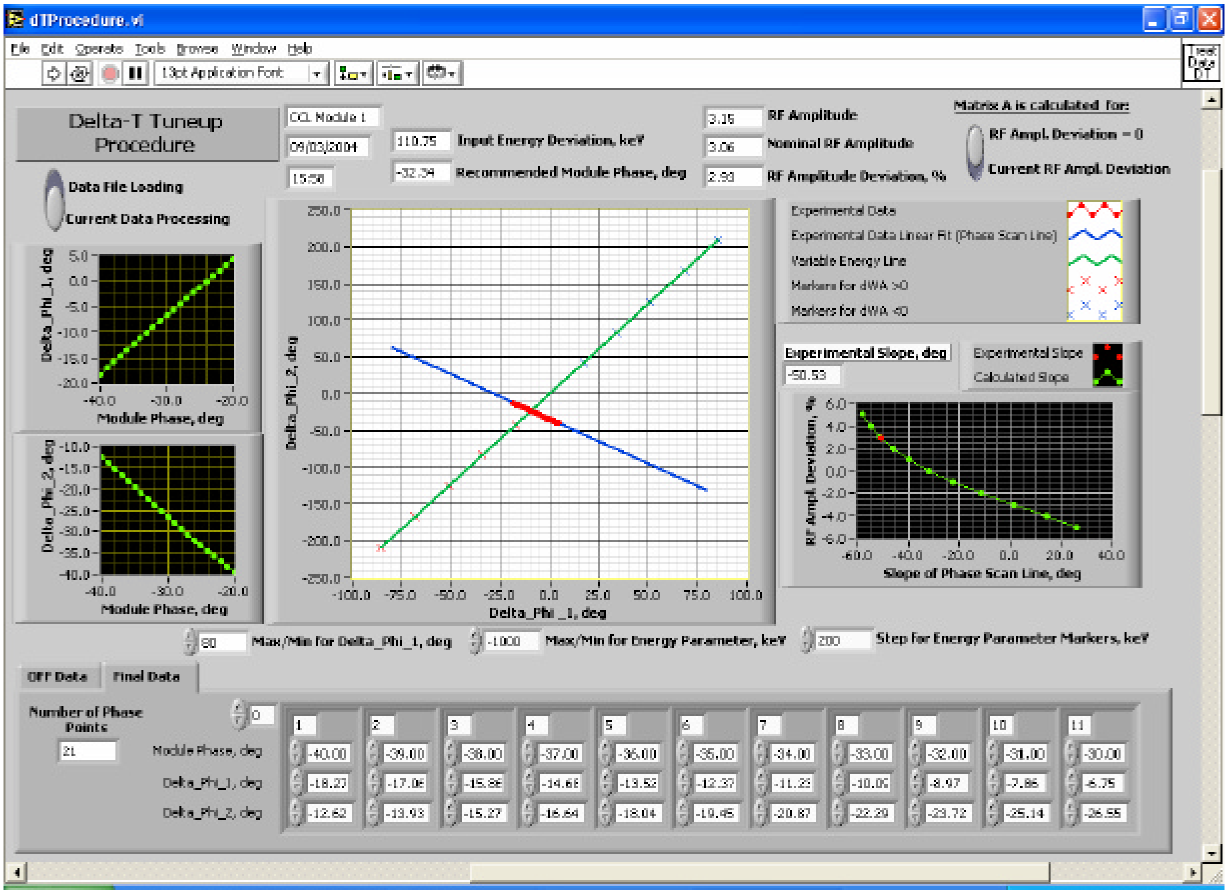

Fig. 5 Display of **dTProcedure** Labview 6.1 program window

corresponding fitting line as well as a theoretical line (2). The plot in the right part of the window represents a calculated relation of slope angle $arctg\left(\frac{d(\Delta j_2)}{d(\Delta j_1)}\right)$ and the amplitude. Experimental value in this plot is indicated as a red spot.

The result of data treatment is the input energy deviation, the recommended nominal module phase and the nominal amplitude.

Matrix elements used for data processing can be selected either for nominal amplitude or for current experimentally found value.

Experimental data are displayed in tables **Final Data** and **OFF Data**. The window also includes the tables with calculated parameters. These tables can be hided to restrict access to calculated parameters. To hide/show the tables click **Show Diagram** in **Window** menu. In the left part of the **dTProcedure.vi Diagram** find **Invariable Parameters** and **Parameters (dE/E)**. Click with right mouse button and select **Hide Control** or **Show Control**.

There is a possibility to display several experimental data sets in a *(?f $_1$, ?f $_2$)* plane in an additional window. Select **Show VI Hierarchy** from **Browse** menu. Double click on ? **gr** box. Additional **t1.vi** window with a *(?f $_1$, ?f $_2$)* plane is opened. Experimental points and fitting lines are accumulated in this window for subsequent executions of **dTProcedure.vi** program.

Figures 6 and 7 demonstrate initial results of setting of amplitude and phase in CCL Modules #1and #2. Preliminary analysis of experimental results shows that random errors essentially depend on stability of accelerator and beam parameters. With the existing stability the errors is estimated to be within ±1% for amplitude, ±1°÷2° for phase and ±10÷20 keV for energy. As for systematic errors, further studies are required.

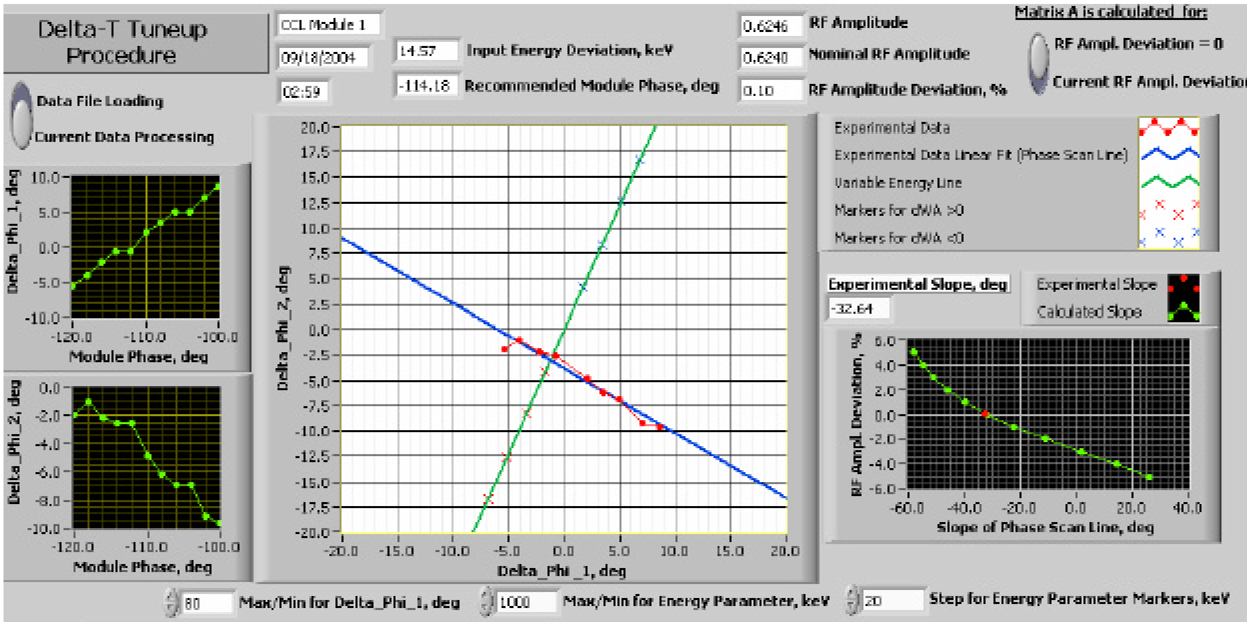

Fig. 6 Results of ? t procedure for CCL Module #1.

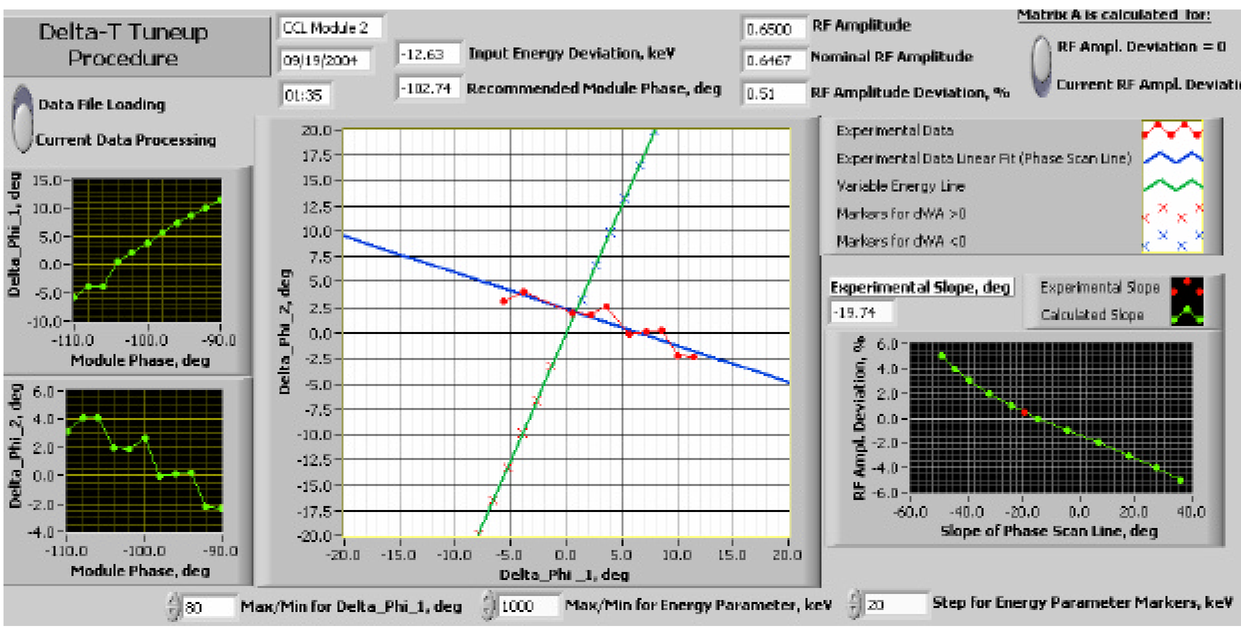

Fig. 7 Results of ? t procedure for CCL Module #2.

References

1. Crandall?????
2. S.V.Dvortsov, A.V.Feschenko, P.N.Ostroumov, S.Z.Zharylkapov. The Δt Procedure Application at the INR Linac, Proc. of the EPAC-3 Conf., Berlin, 24-28 March, 1992, v. 2, pp. 1209-1211.